

Contract No:

This document was prepared in conjunction with work accomplished under Contract No. DE-AC09-08SR22470 with the U.S. Department of Energy.

Disclaimer:

This work was prepared under an agreement with and funded by the U.S. Government. Neither the U. S. Government or its employees, nor any of its contractors, subcontractors or their employees, makes any express or implied: 1. warranty or assumes any legal liability for the accuracy, completeness, or for the use or results of such use of any information, product, or process disclosed; or 2. representation that such use or results of such use would not infringe privately owned rights; or 3. endorsement or recommendation of any specifically identified commercial product, process, or service. Any views and opinions of authors expressed in this work do not necessarily state or reflect those of the United States Government, or its contractors, or subcontractors.

A Study of Grout Flow Pattern Analysis

S. Y. Lee and S. Hyun*

Computational Sciences

Savannah River National University, Aiken, SC 29808

(803)725-8462 si.lee@srnl.doe.gov,

*Mercer University, Macon, GA 31207

HYUN_S@mercer.edu

Abstract - A new disposal unit, designated as Salt Disposal Unit #6 (SDU6), is being designed for support of site accelerated closure goals and salt nuclear waste projections identified in the new Liquid Waste System plan. The unit is cylindrical disposal vault of 380 ft diameter and 43 ft in height, and it has about 30 million gallons of capacity. Primary objective was to develop the computational model and to perform the evaluations for the flow patterns of grout material in SDU6 as function of elevation of grout discharge port, and slurry rheology. A Bingham plastic model was basically used to represent the grout flow behavior. A two-phase modeling approach was taken to achieve the objective. This approach assumes that the air-grout interface determines the shape of the accumulation mound. The results of this study were used to develop the design guidelines for the discharge ports of the Saltstone feed materials in the SDU6 facility. The focusing areas of the modeling study are to estimate the domain size of the grout materials radially spread on the facility floor under the baseline modeling conditions, to perform the sensitivity analysis with respect to the baseline design and operating conditions such as elevation of discharge port, discharge pipe diameter, and grout properties, and to determine the changes in grout density as it is related to grout drop height. An axi-symmetric two-phase modeling method was used for computational efficiency. Based on the nominal design and operating conditions, a transient computational approach was taken to compute flow fields mainly driven by pumping inertia and natural gravity. Detailed solution methodology and analysis results are discussed here.

I. INTRODUCTION

A new disposal unit, designated as Salt Disposal Unit 6 (SDU6), is being designed for support of site accelerated closure goals and salt waste projections identified in the new liquid waste system plan. The unit is a cylindrical disposal vault of 375 ft (average) in diameter and 43 ft in height, and it has a minimum 30 million gallons of capacity. Savannah River National Laboratory (SRNL) evaluated an increased grout placement height and determine whether grout quality is impacted. The primary goals are to develop the baseline Computational Fluid Dynamics (CFD) model and to perform the evaluations for the flow patterns of grout material in SDU6 as a function of elevation of grout discharge port and grout rheology. The modeling domain is schematically shown in Fig. 1. A Bingham Plastic flow model is used as a baseline performance analysis to represent the grout flow behavior for the SDU6 facility. A two-phase modeling approach is taken by considering two fluids of air and grout for the entire space of the facility. In this case, the grout fluid is modeled as a single-phase homogeneous mixture. This approach assumes that the air-grout interface will determine the shape of the accumulation mound. A transient method is used to simulate sequential pours on top of accumulated material.

The SDU6 Engineering Team has identified a technical gap for the increased grout placement height and its impact on grout quality. A CFD simulation study was performed to evaluate the flow pattern behavior driven by flow impingement and gravity along the horizontal floor and to estimate the grout flow radius from the pour location in SDU6. The grout flow radius

is designated as the parameter r in Fig. 1. The results of this study will be used to develop the design guidelines for the SDU6 grout discharge ports.

The objectives of the simulation study are to:

- Estimate the domain size of the grout materials radially spread on the facility floor under the baseline modeling conditions as shown in Table 1.
- Perform the sensitivity analysis with respect to the baseline design and operating conditions such as elevation of the discharge port and fresh grout properties.
- Determine the changes in grout density as it is related to grout drop height.

A three-dimensional CFD two-phase modeling method with a symmetric boundary is used for computational efficiency to achieve the objectives.

II. MODELING APPROACH AND SOLUTION METHOD

The modeling simulations was made by solving transient two-component air-grout, isothermal governing equations with a volume-of-fluid (VOF) method to compute radial flow fields spread on the horizontal floor when 150 gpm grout flow through a 3-inch pipe is poured into 375 ft cylindrical vault at different elevations as shown in Fig. 1.

The VOF model can model two or more immiscible fluids by solving a single set of momentum equations and tracking the volume fraction of each of the fluids throughout the domain. The VOF formulation relies on the fact that two fluids of air and grout are not interpenetrating. For each phase, a variable is

introduced as the volume fraction of the phase in the computational cell. In each control volume, the volume fractions of two phases sum to unity. Based on the local value of grout volume fraction, the appropriate properties and variables is assigned to each control volume within the domain. The VOF model also considers the effects of surface tension of grout against air along the interface.

Hydraulic flow regime conditions were determined by estimating the Reynolds number corresponding to the operating conditions of a grout pouring rate considered for the Saltstone modeling study. The flow domain driven by the nominal flowrate of 150 gpm through 3 inch pipe is laminar-turbulent transition in terms of Reynolds number (~4,500). For the analysis, a standard two-equation turbulence model, referred to as the κ - ϵ model in the literature, is used to capture turbulent eddy motion due to the grout impingement on the floor. When air and grout components are homogeneously mixed in each of the computational cells for the VOF model, equation of the mixture momentum is

$$\frac{\partial(\rho\vec{v})}{\partial t} + \nabla \cdot (\rho\vec{v}\vec{v}) = -\nabla P + (\nabla \cdot \tau) + \rho\vec{g} \quad (1)$$

The shear force term in Eq (1) becomes

$$(\nabla \cdot \tau) = \mu \nabla \cdot (\nabla \vec{v}) = \mu \nabla (\nabla \cdot \vec{v}) - \mu \nabla \times \vec{\Omega} \quad (2)$$

It is noted that the shear term drives fluid rotation as shown in the second term of the right hand side in Eq. (2). The shear term on the right hand side of the equation requires fluid viscosity.

The viscosity is the ability of a material to resist flow. A higher viscosity is characteristic of a less flowable suspension. Consistency η_{∞} becomes constant under the Bingham plastic model, that is,

$$\tau = \tau_o + \eta_{\infty} \dot{\gamma} \quad (3)$$

The plastic viscosity η_{∞} is found from the slope of the linear portion of the shear rate-shear stress curve. The yield stress τ_o is the minimum stress required for a material to start flowing and deforming.

Most of the non-Newtonian behavior of grout was calculated with a yield stress model with a single phase fluid simulation such as the Bingham plastic model with a typical yield stress. This approach was modified for simulating complex phenomena such as thixotropy, i.e., time-dependent viscosity behavior. The model used for this computational modeling task was proposed by Roussel et al. (2007) by modifying the Bingham plastic model for concrete flow. The model was modified with two additional intrinsic parameters such as the re-structuration rate of the cement mixture at rest and a de-structuration parameter.

The shear stress is defined as Bingham plastic viscosity model

$$\tau = (1 + \lambda)\tau_o + \eta_{\infty} \dot{\gamma} \quad (4)$$

$$\frac{\partial \lambda}{\partial t} = \frac{A_{thix}}{\tau_o} - \alpha \lambda \dot{\gamma} \quad (5)$$

λ is the structuration state of grout that evolves through the flow history. Thus, we calculated the age-of-fluid, i.e., time elapsed after pouring through the nozzle, which can be used for predicting the flow history in a Lagrangian way. From Eqs. (4) and (5), τ can be solved with a zero initial value in terms of age-of-grout (AoG), t_{AoG} . The concept of AoG is similar to the residence time of fluid.

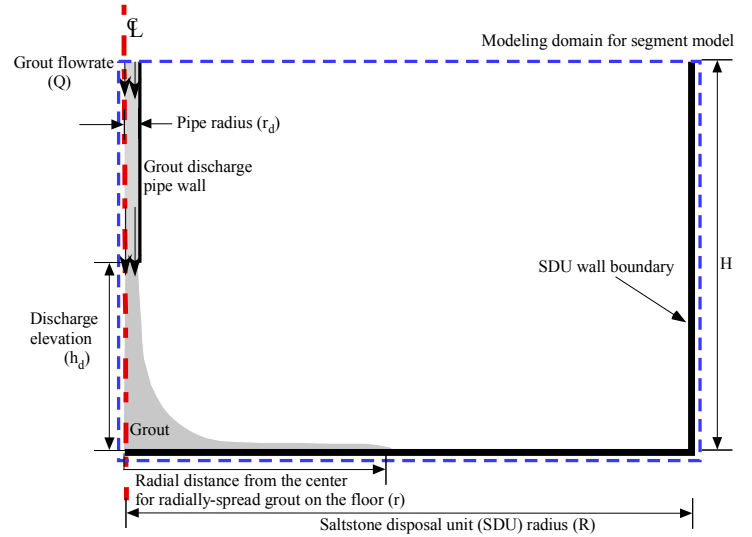


Figure 1. Axi-symmetric configurations of SDU6 for the analysis

Table 1. Nominal operating conditions for the analysis

Parameters		Modeling input
SDU6 facility	Diameter in average	375 ft
	Diameter / Height (H)	375 ft / 43 ft
Grout discharge	Pipe exit radius (r_d)	1.5 in
	Discharge elevation (h_d)	43 ft – maximum (nominal: 5 ft and 43 ft) (Discharge point elevation range: 5 ft to 43 ft)
	Grout discharge flowrate (Q)	150 gpm
	Average grout velocity at pipe exit	6.808 ft/sec
Material properties	Specific gravity	1.63 ~ 1.74 (nominal: 1.7)
	Apparent viscosity	40 ~ 203 cp (nominal: 60 cp*, 120 cp)
	Yield stress	2~11 Pa (nominal: 5 Pa)
	Surface tension (N/m)	0.06

Note:*Viscosity corresponding to 25 wt% salt solution

$$\tau = \tau_o + \left\{ \eta_\infty + \frac{A_{thix}}{\delta(\dot{\gamma})^2} (1 - e^{-\delta\dot{\gamma}t_{AoG}}) \right\} \dot{\gamma} \quad (6)$$

The age-of-grout (AoG), t_{AoG} with time scale unit [second], is obtained from the following convective-diffusive transport equation:

$$\frac{\partial(t_{AoG})}{\partial t} + \frac{\partial(u_i t_{AoG})}{\partial x_i} - \frac{\partial}{\partial x_i} \left[\left(\frac{\nu}{Sc} + \frac{\nu_t}{Sc_t} \right) \frac{\partial t_{AoG}}{\partial x_i} \right] = S_\tau \quad (7)$$

where u_i is the i -directional velocity component; ν and ν_t are the laminar and turbulent kinematic viscosities, respectively; Sc is the laminar Schmidt number of a fluid; Sc_t is the turbulent Schmidt number for the t_{AoG} ; and S_τ is the source of the t_{AoG} . Using $\overline{t_{AoG}}$ instead of t_{AoG} , Eq. (10) can be modified as follows:

$$\frac{\partial(\overline{t_{AoG}})}{\partial t} + \frac{\partial(u_i \overline{t_{AoG}})}{\partial x_i} - \frac{\partial}{\partial x_i} \left[\left(\frac{\nu}{Sc} + \frac{\nu_t}{Sc_t} \right) \frac{\partial \overline{t_{AoG}}}{\partial x_i} \right] = 1.0 \quad (8)$$

where $\overline{t_{AoG}}$ is equal to t_{AoG} / S_τ . For this case, S_τ is 1, and the $\overline{t_{AoG}}$ is equal to t_{AoG} .

For the solution of the local t_{AoG} indicator Eq. (8), the boundary conditions are zero [second] at the inlet and zero gradients at the exit and the wall, and the initial condition is set equal to zero [second] for the whole flow field. The t_{AoG} is a passive quantity and does not affect fluid flow patterns. From Eq. (6) viscosity can be estimated as function of shear rate as well as aging of grout, t_{AoG} . For the scoping calculations, the modeling constants in Eq. (6), A_{thix} and δ , are assumed to be 0.01 Pa/sec and 0.1, respectively, according to the literature information [Roussel et al., 2007].

The analysis consists of two major parts. One part is to estimate the radial distance from the pouring point by applying the Bingham plastic model to the computational domain. The second part is to apply the Bingham plastic methodology to modeling the aging fluid simulations to evaluate the impact of fluid aging on the grout flow performance of the SDU6 for two different consistencies.

The transient governing equations as described previously were solved simultaneously by using a commercial CFD code, FluentTM. The analyses were based on the 10° pie-type segment model for computational efficiency as shown in Fig. 2.

The main solution methodologies and modeling assumptions were as follows:

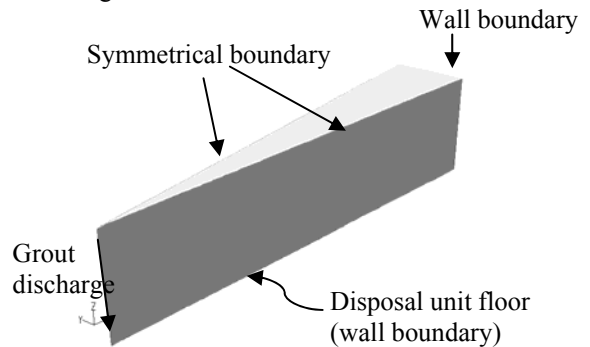
- The temperature is isothermally kept at 75 °F, neglecting the hydration heat generation of the cementitious material during the pouring process.

- For the analysis of two-component flow consisting of air and grout, the grout material is treated as a single-phase homogeneous fluid.
- The fluid behavior follows the Bingham plastic model.
- The model was based on 375-ft cylindrical vault with no internal solid structures.
- Top fluid surface is at atmospheric pressure.

In summary, the governing equations to be solved by the CFD approach are one continuity equation, three air-grout mixture momentum equations for the three component directions (x , y , and z directions). As a constitutive relation, the Bingham plastic model or the grout aging model is used to estimate the viscous shear stress for the SDU6 domain, assuming that it would give an acceptable representation of the grout material characteristics. The sensitivity studies are performed using typical yield stress for different viscosities and different elevations of the grout discharge port.

Transient numerical simulations are made for the Saltstone modeling study by taking two modeling approaches. One is the baseline model for a simple Bingham plastic model to perform the initial scoping calculations of the flow patterns and domain size radially spread for different operating conditions. The other is the grout aging model to evaluate the aging impact of the viscous grout materials on the size of the radial spreading of the grout for various operating conditions.

The number of the established computational meshes for the modeling domain shown in Fig. 2 is about 2×10^5 nodes. This number was established from sensitivity studies of computational meshes, verifying that the mesh size is independent of the solutions within about 1% deviations. Mesh density is significantly higher in the vicinity of the pouring point on the vault floor to capture the high-speed impinging flow behavior related to the air entrainment. A range of operating conditions such as different viscosities and grout discharge elevations was considered to perform the sensitivity calculations for the flow patterns with respect to the baseline modeling results.



(Computational modeling domain for 10° sector model)

Figure 2. Computational domain used for the baseline modeling calculations

III. RESULTS AND DISCUSSIONS

For the modeling calculations, Bingham plastic and time-dependent grout models were considered for examining the impact of fluid spread performance for the initial baseline configurations. As the performance criteria, the shear rate profile and air contents within the grout material were used as a key indicator of the grout flow movement from the grout pouring region toward the remote wall boundary zone on the facility floor. If the local shear rate for the grout materials gets smaller than 10^{-3} (1/sec), the materials will not be moved adequately and may be eventually solidified. Estimation of flow patterns was used as the degree of grout pouring efficiency from the pouring center to the front edge of the layer. The grout layer accumulated on the floor was estimated from the flow domain of the feed materials obtained by the VOF method for each cell of the computational domain along the fluid movement starting from the material feed inlet. In the analysis, the grout quality was estimated in terms of the grout density formed on the facility floor. Radial spread distance was estimated from the center of grout pouring to the point at which grout volume fraction is higher than 0.1. Benchmarking analysis of the modeling predictions against experimental results is not included here because of limited paper space.

III.A. BINGHAM PLASTIC MODELING RESULTS

A Bingham plastic model with 5 Pa yield stress and 60 cp consistency was used for the baseline analysis for basic flow patterns and characteristics associated with radial grout spreading. Based on the domain and operating conditions as shown in Fig. 1 and Table 1, transient VOF modeling calculations were performed on the SRNL High Performance Computing (HPC) platform to compute grout flow fields when a 150 gpm flowrate was poured down through a 3-inch pipe at two different elevations, 5 and 43 feet, above the SDU6 floor. Typical computational time was about 6 weeks for the first one-hour transient modeling simulation on a 4 CPU parallel HPC platform. Following the first hour of simulation, another one-hour simulation took about 3 weeks due to the increased time step size required for numerical convergence.

The transient results for the Bingham plastic model show that an uneven top surface of the grout layer accumulated around the pouring center of the disposal unit floor is established in about 30 minutes' pouring time. When grout material is poured down at 150 gpm flowrate, 6.81 ft/sec velocity, through a 3 in discharge pipe from 5 feet above the floor, the results show that the grout layer for 5 ft pouring height has smooth surface except for the central region of about 2 ft radial distance from the impinging point on the dry SDU6 floor.

When grout is pouring down from the different heights of 5 ft and 43 ft above the disposal floor, the modeling results show that when heavy grout material of 1.7 g/ml is pouring down toward the floor of the disposal unit, maximum speeds of about 6 m/sec for a 5 ft pouring height and 16 m/sec for a 43 ft height

are reached just before grout impingement on the floor. Thus, when the grout discharging port becomes higher, the grout impinging speed on the disposal floor becomes higher as expected. It is clearly indicated that rough grout surface is formed near the central spot of the pouring because of high impinging speed of the grout material on the facility floor. As a grout layer accumulated on the floor of storage vault becomes higher with pouring time increased, grout splashing and impinging on the floor can result in air being drawn into the grout zone of the layer as shown in the figures. This can cause degradation of grout quality for the accumulation layer.

When grout pouring time increases, the grout materials are continuously accumulated near the center of pouring, resulting in a more smooth shape of the mound layer. Table 2 quantitatively compares thicknesses of the grout accumulation layer between the two discharge heights of 5 and 43 feet at a 3-ft radial distance from the pouring center for various pouring times. It is noted that when a grout flow of 150 gpm discharges downward at the 43 ft height, the accumulated layer near the impinging point is established smoothly after the 1 hour transient time, and its layer thickness and shape become very similar to those of the 5 ft discharge case.

The impact of different grout pouring heights on the grout quality for the layer accumulated on the SDU6 floor was evaluated by grout volume fraction for the present preliminary work. Table 3 shows quantitative comparison of transient grout volume fractions for the grout layer for the two different pouring heights of 5 ft and 43 ft.

The baseline results for the 5 ft pouring height show that when the 150 gpm grout flow with a 5 Pa yield stress and a 60 cP viscosity is poured down through a 3-in discharge port, the grout is spread radially up to about 64 ft distance from the pouring center after 2 hours' pouring time. The air volume of the grout layer for 5 minutes' transient time has about 71% at 5 minutes' transient time, and it is reduced by about 9% in 2 hours' pouring time, resulting in the nominal grout density consisting of about 80% grout and 20% air volume fractions. The sensitivity results clearly indicate that the radial spread for the 43 ft discharge port is about 10% faster than that of the 5 ft discharge port for the early transient period of 5 minutes. It is noted that when the pouring height for 150 gpm flow increases from 5 ft to 43 ft, the grout layer formed during the early transient period contains void volume about 10% higher than the lower pouring height as shown in Table 3. However, for the pouring time longer than half an hour, an increased grout height placement has an insignificant impact on the radial spread rate and the trapped air volume associated with grout quality as shown in Table 3.

Table 2. Comparison of transient accumulation thickness on the SDU floor for two different pouring heights.

Pouring height (feet)	Layer thickness* accumulated on the floor at 1-meter radial distance for different pouring times (inches)			
	5 min.	30 min.	1 hr	2 hrs
5	0.60	1.04	2.44	2.54
43	1.22	1.53	2.44	2.54

Note:* Defined as the height where grout volume fraction is higher than 99%

Table 3. Comparison of transient grout volume fractions for the grout layer on the SDU floor for two different pouring heights.

Pouring height (feet)	Grout volume fractions* for the grout layer accumulated on the floor at 1-meter radial distance for different pouring times			
	5 min.	30 min.	1 hr	2 hrs
5	0.71	0.78	0.79	0.80
43	0.66	0.74	0.78	0.80

Note:* Defined as the area-averaged volume fractions for grout height where grout volume fraction is higher than 10% at 1-m radial distance

III.B. GROUT AGING MODELING RESULTS

The modified Bingham plastic behavior of grout such as thixotropy, i.e., time-dependent viscosity behavior, was modified for conducting the initial scoping calculations to assess the impact of fluid aging on radial spreading and basic flow patterns. The model was proposed by Roussel et al. (2007) by modifying the Bingham plastic model for concrete flow, referred to as the Grout Aging Model in this report. The modified model includes two additional intrinsic parameters: the structuration rate of the cement mixture at rest and a de-structuration parameter. The structuration state of grout evolves through the flow history. Thus, we calculated the age-of-fluid, i.e., time elapsed after pouring through the nozzle, which can be used for predicting the flow history in a Lagrangian way. From Eq. (8), the structuration rate λ was calculated with zero initial value in terms of fluid residence time. For the calculations, thixotropic and transient constants related to the structuration rate are 0.01 Pa/sec and 0.1, respectively.

At the beginning of the pouring process (i.e., $t < 20$ seconds), it is required to have a smaller time step (i.e., 1.0×10^{-4} seconds) to achieve a stable converging simulation. However, it was possible to increase time steps when the grout flow was established including impingement of the grout on the bottom floor of the tank and the grout splashing in a radial direction. For the modeling analysis, continuity, momentum, turbulent kinetic energy, and vorticity equations were solved. In addition, the age of the grout was calculated using a convective-diffusive equation with zero diffusivity to calculate the time-dependent viscosity. Total CPU hours for transient simulation up to 1800 seconds took about 360 CPU hours.

A sensitivity analysis for grout pouring height and viscosity under the aging fluid model was performed. Transient radial distances from the pouring point are compared for two different pouring heights of 5 ft and 43 ft above the disposal unit floor under two different non-Newtonian models of idealized Bingham plastic model and grout aging model as shown in Fig. 3. The results show that when values of 0.01 Pa/sec for the thixotropic constant and 0.1 for the viscosity time constant in Eq. (9) are used, the overall transient behaviors for the two models are similar, but the thixotropic grout aging model predicts a radial distance about 10% higher than the idealized Bingham plastic model during the first half an hour period.

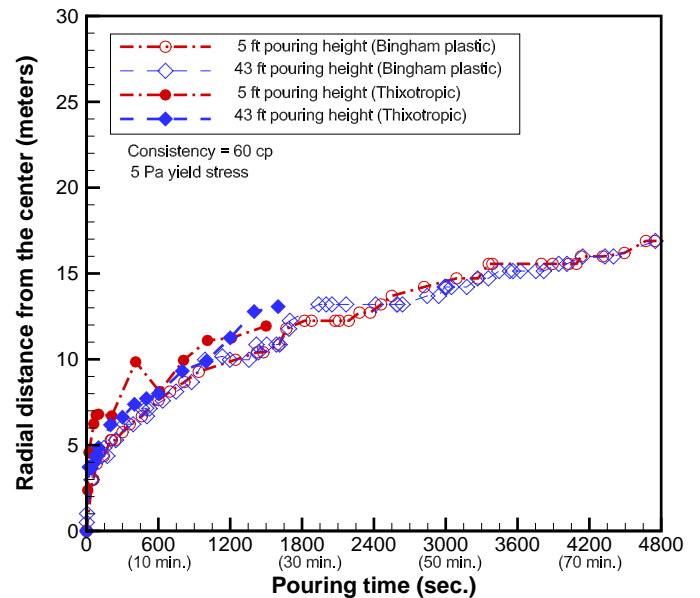


Figure 3. Comparison of transient radial distances from pouring point for two different pouring heights (5 ft and 43 ft elevations) under two different non-Newtonian models.

When grout viscosity increases from 60 cp to 120 cp for two different pouring heights (5 ft and 43 ft elevations) under the thixotropic model, the radial spread rate for the higher viscosity grout is much slower than that of the lower viscosity grout. When the fresh grout viscosity increases from 60 cp to 120 cp for a fixed pouring height of 5 ft above the disposal floor, the thickness of the layer accumulated on the floor becomes higher because of the increased viscosity. The transient modeling results clearly show that when the grout becomes more viscous, the thickness of the grout layer accumulated on the floor becomes higher and the radial spread distance becomes smaller because of the slower movement. It is noted that as grout becomes more viscous, average void volume for the grout layer at a given radial distance becomes smaller for the slower movement along the radial direction.

IV. CONCLUSION

As the performance criteria, shear rate profile and air contents within the grout material were used as key indicators of the grout flow movement from the grout pouring region toward the remote wall boundary zone on the facility floor. Estimation of flow patterns was used as the degree of grout pouring efficiency from the pouring center to prevent uneven mound formation.

Recommended operational guidance was developed assuming that local shear rates and flow patterns related to radial spread along the SDU floor can be used as a measure of grout performance and spatial dispersion affected by the grout height and viscosity. The grout quality was estimated in terms of the grout volume fractions formed on the facility floor, leading to the change of grout density.

The main conclusions drawn from the grout modeling and calculations are as follows:

- The baseline results for the 5 ft pouring height show that when the 150 gpm grout flow with a 5 Pa yield stress and a 60 cp viscosity is poured down through a 3-in discharge port, the grout is spread radially up to about 64 ft distance from the pouring center after 2 hours' pouring time. The air volume fraction of the grout layer is about 29% at 5 minutes' transient time, and it is reduced by about 9% in 2 hours' pouring time, resulting in the grout density consisting of about 80% grout and 20% air volume fractions.
- The sensitivity results show that when the discharge port is located at a higher position, a larger amount of air is trapped inside the layer formed below the discharge port at the early transient time of less than 30 minutes because of the higher impinging momentum of the grout flow on the floor, resulting in the formation of less smooth layer.
- The results clearly indicate that the radial spread for the 43 ft discharge port is about 10% faster than that of the 5 ft discharge port for the early transient period of 5 minutes.

However, for the pouring time longer than half an hour, the discharge port height does not affect the radial distance spread on the disposal floor.

- The sensitivity results show that for 150 gpm grout flow from 43 ft height above the floor, the grout layer formed during the early transient period contains the void volume about 10% higher than the lower pouring height of 5 ft. However, for the pouring time longer than half an hour, the discharge port height has insignificant impact on the trapped air volume related to the grout quality.
- The results for the transient viscosity model show that when grout material becomes more viscous, the thickness of the grout layer accumulated on the floor becomes higher, but the radial distance spread on the horizontal floor becomes smaller. The early transient results for the grout density with about 32% air volume fractions are in reasonable agreement with those of the idealized Bingham plastic model.

It is recommended that the current models developed here be benchmarked against the experimental results for critical applications of the modeling results.

REFERENCES

1. A. D. Cozzi, E. K. Hansen, T. M. Jones, and Y. R. Safford, "Bench Scale Saltstone Process Development Mixing Study", SRNL-STI-2011-00346, Revision 0, June 2011.
2. S. Y. Lee, R. A. Dimenna, R. A. Leishear, D. B. Stefanko, "Analysis of Turbulent Mixing Jets in a Large Scale Tank", *ASME Journal of Fluids Engineering*, Volume 130, Number 1, pp. 011104, 2008.
3. *FLUENT*, Fluent, Inc., 2003
4. R. A. Leishear, S. Y. Lee, M. D. Fowley, M. R. Poirier, T. J. Steeper, "Comparison of Experiments to Computational Fluid Dynamics Models for Mixing Using Dual Opposing Jets in Tanks With and Without Internal Obstructions", *ASME J. of Fluids Engineering*, vol. 134, pp. 111102, November 2012.
5. Roussel N., Geiker M.R., Dufour F., Thrane L.N., and Szabo, P., "Computational modeling of concrete flow: General overview," *Cement and Concrete Research*, 37, pp 1298-1307, 2007.